Encapsulation of segmented Pd–Co nanocomposites into vertically aligned carbon nanotubes by plasma-hydrogen-induced demixing

Takeshi Fujita
International Frontier Center for Advanced Materials, Institute for Materials Research, Tohoku University, Aoba-ku, Sendai, Miyagi 980-8577, Japan

Yasuhiko Hayashi[a)]
Department of Environmental Technology and Urban Planning, Nagoya Institute of Technology, Gokiso, Showa, Nagoya 466-8555, Japan

Tomoharu Tokunaga
Department of Materials Science and Engineering, Faculty of Engineering, Kyushu University, Motooka, Nishi-ku, Fukuoka 819-0395, Japan

T. Butler, N. L. Rupesinghe, K. B. K. Teo, and G. A. J. Amaratunga
Department of Engineering, University of Cambridge, 9 JJ Thomson Avenue, Cambridge CB3 0FA, United Kingdom

(Received 27 December 2006; accepted 26 February 2007; published online 29 March 2007)

Vertically aligned carbon nanotubes (VA-CNTs) filled with Pd–Co nanocomposites on an Si substrate have been synthesized by microwave plasma-enhanced chemical vapor deposition. It was confirmed that adjacent Pd–Co nanocomposites in the VA-CNTs were compositionally separated. Most CNTs contained Co pillars on top; however, Pd pillars were rarely present. The strong magnetic induction from an individual Co pillar was revealed by electron holography. The simultaneous phenomenon of the demixing by plasma hydrogen irradiation and the preferential encapsulation into CNTs realized the unique Pd–Co nanocomposites. © *2007 American Institute of Physics*. [DOI: 10.1063/1.2718268]

Since the discovery of carbon nanotubes (CNTs),[1] several researches aiming toward the encapsulation of metals into CNTs have been carried out. In particular, vertically aligned carbon nanotubes (VA-CNTs) are one of the most important candidate materials for field-emitter arrays in flat-panel displays and high-density recording media. In order to obtain additional functionalities, several catalytic metals or alloys such as Fe, Ni, Co, Cu, and FeCo were chosen to grow CNTs containing metallic nanowires or nanorods by chemical synthesis;[2–4] however, the control of segmented metals in these CNTs could not be achieved as a result of the encapsulation. A well-known technique to produce segmented metallic nanowires is by the combination of an anodized-aluminum-oxide template and electrodeposition with different electrolytes.[5] However, the oxidation in air may significantly degrade the functional property owing to the absence of protective surface layers such as outer-shell CNTs. The advantage of outer-shell CNTs is that the internal nanostructures are well protected from being oxidized at an ambient temperature.[6] Therefore, establishing a technique to encapsulate segmented metals into CNTs is important. In our previous study, either elemental Pd or Co was selected as the encapsulated metal because it functions as a candidate material for hydrogen storage or information storage, respectively. Microwave plasma-enhanced chemical vapor deposition (MPECVD) was employed to grow CNTs filled with Pd and Co.[7,8] In this study, we demonstrate the realization of VA-CNTs filled with segmented Pd–Co nanocomposites and reveal their detailed microstructure, composition, and local magnetic induction by means of transmission electron microscopy (TEM) and related techniques.

The silicon substrate was cleaned for 1 min using hydrofluoric acid, and the substrate surface was oxidized by using an acid solution (H_2SO_4:H_2O_2=4:1). By using a vacuum evaporation method, a primary Pd metal layer (thickness: 6 nm) and a secondary Co metal layer (thickness: 9 nm) were deposited on a thin barrier layer of SiO_2 formed on the Si surface in order to prevent the formation of silicide. The Si substrate was then transferred into the MPECVD system. The inside of the chamber was evacuated to below 10^{-8} Torr. The substrate was then heated to 973 K and maintained in an H_2-gas atmosphere at 50 Torr for 600 s. The microwave plasma hydrogen irradiation was conducted at a frequency of 2.45 GHz and power of 600 W; further, a negative bias of 400 V was applied to the substrate, as described elsewhere.[9] In order to obtain an effective substrate bias, the substrate was placed on a quartz board. The VA-CNTs were grown on the substrate while the feed gas (CH_4) was being introduced at a pressure of 20 Torr for 600 s. Subsequently, the microwave plasma hydrogen irradiation and the negative bias were discontinued and the substrate temperature was then reduced to room temperature in the growth chamber under an H_2-gas atmosphere of 50 Torr.

Pd–Co nanocomposite-filled VA-CNTs were observed on the substrate by using a scanning electron microscope (SEM), Hitachi S-3000. TEM samples with a thickness of approximately 1 mm were carved from the Si substrate and attached to a commercial Mo TEM mesh. The microstructures were observed using a Philips CM200TEM operated at 200 kV and equipped with an electrostatic biprism. X-ray spectra were obtained using a Noran energy-dispersive x-ray spectrometer (EDS) with an ultrathin window.

[a)]Author to whom correspondence should be addressed. Fax: +81(52)735-5104; electronic mail: hayashi.yasuhiko@nitech.ac.jp

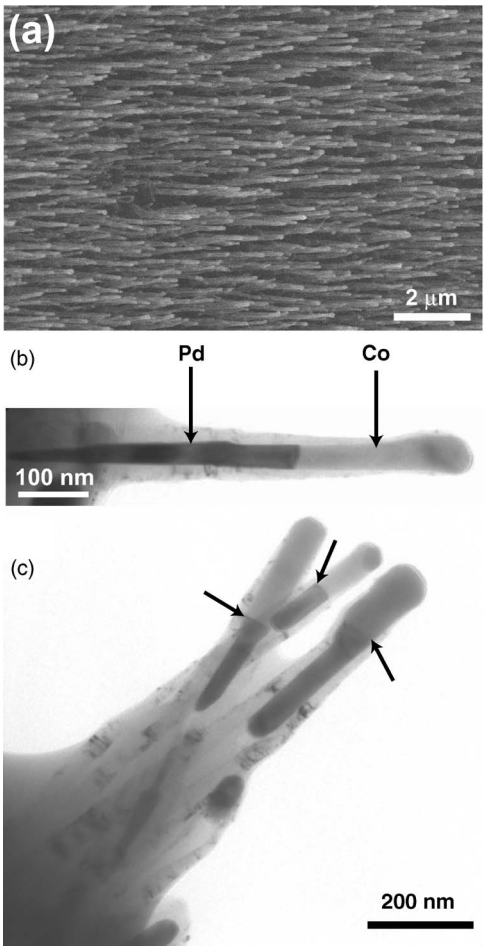

FIG. 1. (a) SEM micrograph of Pd–Co nanocomposite-filled CNTs grown on an Si substrate. The CNTs have a needlelike morphology and are aligned along one direction. Representative TEM bright-field micrographs. (b) Needle tips show the connected Co and Pd metals encapsulated entirely within the CNT. (c) A bundle of CNTs wrapping the segmented Pd–Co nanocomposites. The three arrows indicate the boundary between Co and Pd.

Figure 1(a) shows an SEM micrograph of Pd–Co nanocomposite-filled VA-CNTs grown on an Si substrate. This micrograph shows a needlelike morphology, uniform distribution density, and almost equal length and diameter. Figures 1(b) and 1(c) show representative bright-field images revealing two different contrasts of the metal pillars inside the CNTs. The upper metal pillars (light contrast) were identified as Co and the lower pillars (dark contrast) as Pd, as shown in Fig. 1(b). The three arrows in Fig. 1(c) indicate the boundaries between Co and Pd. The length of the combined metal pillar ranged from 200 to 800 nm. The average length and diameter of the VA-CNTs obtained from the TEM observation were approximately 1 μm and 100 nm, respectively. The CNTs containing these pillars indicated poor crystallization, and the convergent-beam electron diffraction (CBED) technique revealed that most of the Co pillars were single crystals. A CBED pattern obtained from a Co pillar revealed that the crystal had a face-centered-cubic (fcc) structure. The crystal structure of Co is fcc at high temperatures; therefore, the transformation from the fcc to hexagonal closed-pack (hcp) structure did not occur during the rapid quenching performed in the MPECVD growth process. In addition, orientation relationships between the Co and Pd crystals were not observed. EDS spectra were obtained to examine the composition of the inner Co and Pd pillars. The EDS spectrum obtained from a Co pillar, shown in Fig. 2(a), reveals the primary peaks of Co and C and minor peaks of Si, Mo, and Pd. The minor peaks of Si and Mo can be attributed to the x-ray background of the TEM sample. The minor peak of Pd indicates that the Co pillar contains a small amount of Pd—less than 0.1 at. %. On the other hand, the EDS spectrum obtained from a Pd metal [Fig. 2(b)] reveals strong Pd peaks with an Si peak due to the x-ray background; however, a Co peak was not evident. Therefore, the MPECVD process can yield Co pillars connected with Pd pillars without significant compositional mixing during the growth process.

We propose the following model to explain the vertical alignment of segmented Pd–Co nanocomposites inside VA-CNTs, as shown in Fig. 3. After annealing at 973 K followed by the deposition of Pd and Co layers on the Si substrate, the Pd–Co layer is fragmented into nanoparticles [Fig. 3(a)]. In general, the growth mechanism of metal films on oxide layers (e.g., SiO_2) depends on the affinity of the metal to react with oxygen.[10] In our case, the substrate does not get wet and the solid-soluted Pd–Co alloy immediately agglomerates into three-dimensional islands. The microwave plasma hydrogen irradiation promotes the demixing of Co and Pd elements inside the Pd–Co islands due to the presence of hydrogen ions or atomic hydrogen. Pd metals tend to form a hydride because the heat of formation of hydride is +15 kJ/mol H for Co and −20 kJ/mol H for Pd.[11] Therefore, the Co–Pd alloy may decompose into Pd hydride and Co only by hydrogen irradiation at high temperatures [Fig. 3(b)].[12] By considering the diffusion rate discussed earlier,[7] we suppose that both the Co and Pd crystals were in the quasiliquid state when they were assembled and encapsulated into straight VA-CNTs by means of a capillary force. Most CNTs contain Co pillars at the top; however, Pd pillars are rarely present. This implies that the Co metals have a lower viscosity than Pd metals in the quasiliquid state during the encapsulation by the capillary force and/or Co exhibits a higher catalyst performance than Pd. The growth of CNTs is performed via the decomposition of carbonaceous gas molecules (CH_4) on the surface of the Co and Pd pillars by means of catalysis assisted by microwave plasma hydrogen irradiation and the diffusion of carbon atoms through the

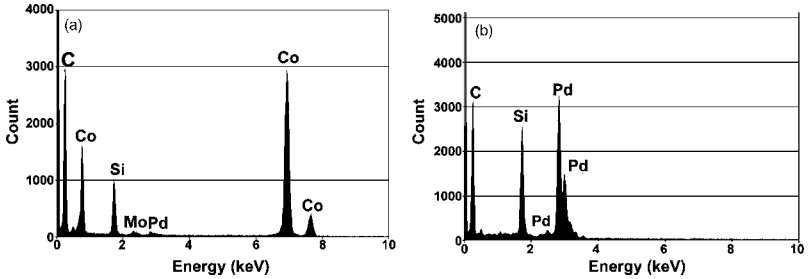

FIG. 2. (a) Typical EDS spectrum obtained from a Co pillar. (b) Typical EDS spectrum obtained from a Pd pillar.

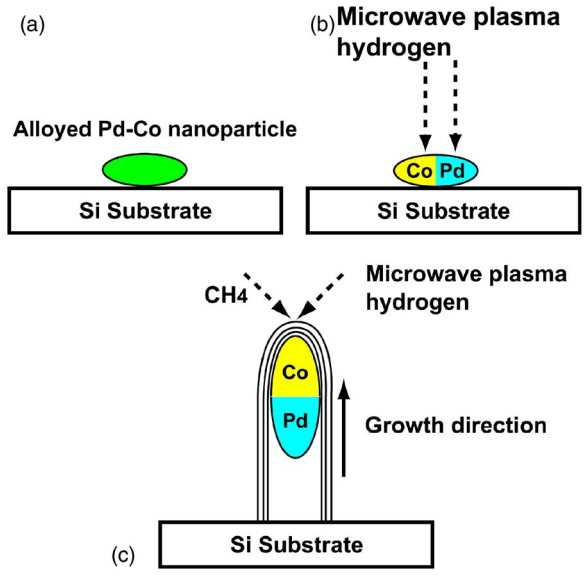

FIG. 3. (Color online) Growth model of the segmented Pd–Co nanocomposites in VA-CNTs. (a) Si substrate with a thin SiO_2 barrier layer and an alloyed Pd–Co nanoparticle. (b) Separated Pd–Co nanoparticle into catalyst by microwave plasma hydrogen irradiation. (c) Decomposition of CH_4 on the catalyst surface.

segmented Pd–Co nanocomposites [Fig. 3(c)]. Overall, the simultaneous phenomenon of demixing by plasma hydrogen irradiation and preferential encapsulation into CNTs can enable the synthesis of segmented Pd–Co nanocomposites encapsulated within VA-CNTs. In addition, we found that the length ratios of the Pd and Co pillars in VA-CNTs are close to the thickness ratios in the case of deposition by the vacuum evaporation method. Further, we verified that different thickness ratios of the deposited layers of Pd and Co, whose total thickness was 15 nm, yielded segmented Pd–Co nanocomposites with almost the same diameter, as shown in Figs. 1(b) and 1(c), and the corresponding length ratios for each segment.

The phase shift in the electron wave obtained from electron holography can be expressed as the sum of the mean inner potential and a magnetic component.[13] Consequently, the local magnetic induction was evaluated by using electron holography. The hologram of an isolated Pd–Co nanocomposite in a CNT and the corresponding magnetic component of the reconstructed phase are shown in Figs. 4(a) and 4(b), respectively. The magnetic induction from the inner Co pillar is clearly evident. This magnetic induction is vertically oriented and thus implies that the Co pillars encapsulated in VA-CNTs may provide potential for further development as vertical recording media. According to the cylindrical model for quantitative electron holography, a component of magnetic induction, $B_{\perp}$, of the Co pillar was estimated to be 1.2 ± 0.1 T, which is the same as the value for the Co pillar without a Pd element for the same MPECVD process.[8] Therefore, the remanent state is independent of the Pd impurity in the Co pillar. Further optimization of the MPECVD process may result in higher values of $B_{\perp}$.

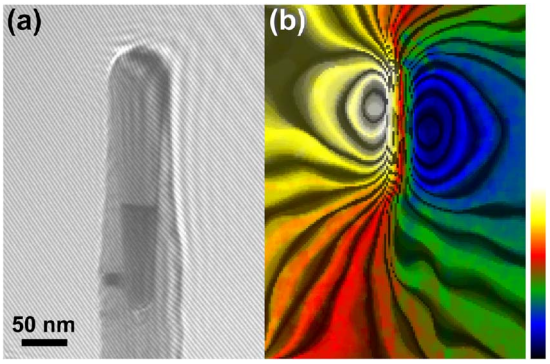

FIG. 4. (Color online) (a) Experimental hologram of the Pd–Co nanocomposite in the CNT. (b) Corresponding color contour map of the magnetic component displaying the magnetic induction emerging from the inner Co pillar.

Pd nanoparticles are excellent hydrogen storage materials,[14] and electron holography has revealed that encapsulated Co pillars exhibit strong magnetic signals. Therefore, the encapsulated Pd–Co nanocomposites developed in this study are multifunctional. The implementation of simultaneous demixing and preferential encapsulation of various materials into VA-CNTs by using the MPECVD process can create frontiers for material sciences and develop applications in fields such as medical sciences, biology, catalysis, and information storage.

The authors would like to thank Professor M. R. McCartney for her valuable comments. This study was supported by the JSPS Postdoctoral Fellowship for Research Abroad and a Grant-in-Aid for Scientific Research (Houga-16651065). The authors gratefully acknowledge the use of facilities in the John M. Cowley Center for High Resolution Electron Microscopy at Arizona State University.

[1] S. Iijima, Nature (London) **354**, 56 (1991).
[2] Y. Saito, T. Yoshikawa, M. Okuda, N. Fujimoto, K. Sumiyama, K. Suzuki, A. Kasuya, and Y. Nishina, J. Phys. Chem. Solids **54**, 1849 (1993).
[3] G. Y. Zhang and E. G. Wang, Appl. Phys. Lett. **82**, 1926 (2003).
[4] A. L. Elías, J. A. Rodríguez-Manzo, M. R. McCartney, D. Golberg, A. Zamudio, S. E. Baltazar, F. López-Urías, E. Muñoz-Sandoval, L. Gu, C. C. Tang, D. J. Smith, Y. Bando, H. Terrones, and M. Terrones, Nano Lett. **5**, 467 (2005).
[5] S. R. Nicewarner-Peña, R. G. Freeman, B. D. Reiss, L. He, D. J. Peña, I. D. Walton, R. Cromer, C. D. Keating, and M. J. Natan, Science **294**, 137 (2001).
[6] T. Fujita, M. W. Chen, X. M. Wang, B. S. Xu, K. Inoke, and K. Yamamoto, J. Appl. Phys. **101**, 014323 (2007).
[7] S. Toh, K. Kaneko, Y. Hayashi, T. Tokunaga, and W.-J. Moon, J. Electron Microsc. **53**, 149 (2004).
[8] T. Fujita, Y. Hayashi, T. Tokunaga, and K. Yamamoto, Appl. Phys. Lett. **88**, 243118 (2006).
[9] Y. Hayashi, T. Tokunaga, T. Jimbo, Y. Yogata, S. Toh, and K. Kaneko, Appl. Phys. Lett. **84**, 2886 (2004).
[10] J. D. Carey and S. R. P. Silva, Nanotechnology **14**, 1223 (2003).
[11] R. Griessen and T. Riesterer, in *Hydrogen in Intermetallic Compounds I*, edited by L. Schlapbach (Springer, Berlin, 1988), p. 219.
[12] T. Tokunaga, Y. Hayashi, T. Fujita, S. R. P. Silva, and G. A. J. Amaratunga, Jpn. J. Appl. Phys., Part 2, **45**, L860 (2006).
[13] A. Tonomura, *Electron holography*, 2nd ed. (Springer, Berlin, 1999), p. 99.
[14] L. L. Jewell and B. H. Davis, Appl. Catal., A **310**, 1 (2006).